Preparation and Catalytic Performances of Ultralarge-Pore TiSBA-15 Mesoporous Molecular Sieves with Very High Ti Content

A. Vinu,*,† P. Srinivasu,‡ M. Miyahara,§ and K. Ariga§

International Center for Young Scientists (ICYS), National Institute for Materials Science (NIMS), 1-1 Namiki, Tsukuba 305-0044, Japan, Division of Materials Science and Chemical Engineering, Yokohoma National University, Yokohoma 240-8501, Japan, and Supermolecules Group, Advanced Materials Laboratory (AML), National Institute for Materials Science (NIMS), 1-1 Namiki, Tsukuba 305-0044, Japan

Received: October 13, 2005; In Final Form: November 10, 2005

Highly ordered TiSBA-15 mesoporous molecular sieves with different n_{Si}/n_{Ti} ratios and tunable pore diameters have been prepared through direct synthesis under various hydrochloric acid concentrations and synthetic temperatures. The structure and the textural parameters of the materials were investigated by powder X-ray diffraction and nitrogen adsorption/desorption measurements. Decrease of the acid concentration and n_{Si}/n_{Ti} ratio in the synthetic gel enhanced the amount of Ti incorporation in SBA-15 materials without affecting their structural order and textural parameters. Highly ordered mesoporous TiSBA-15 with a very high Ti content up to a n_{Si}/n_{Ti} ratio of 1.9 was prepared for the first time under the optimized synthesis conditions. Control of synthetic temperature resulted in tuning of pore geometries without structural deterioration and Ti content. Ultralarge-pore TiSBA-15 with a pore size of 12.6 nm and a pore volume of 1.3 $cm^3\ g^{-1}$ was also synthesized. The nature and the coordination of the Ti atoms in SBA-15 prepared under various synthesis conditions were investigated by UV−vis spectroscopy. It has been found that the Ti atoms are well-dispersed and mostly occupy the tetrahedral coordination under the optimized synthesis conditions. Catalytic performance of the obtained TiSBA-15 materials was also investigated through oxidation of styrene by hydrogen peroxide and *tert*-butylhydroperoxide as oxidants.

Introduction

Mesoporous materials have attained considerable attention in the recent years because of their large surface area, pore volume, and uniform pore size distribution, and their good performances as effective biological adsorbents and catalysts in processes which allow easy diffusion of large-size organic molecules to internal active sites. The discovery of the new family of mesoporous silica molecular sieves with pore diameters in the range of 2.0−10.0 nm, designated as M41S, was reported by Beck and co-workers, is of considerable interest for heterogeneous catalysis and material science.[1,2] Among mesoporous silica materials, the hexagonally ordered large-pore SBA-15 is currently paid much attention due to its easy synthesis, tunable pore size, thick pore wall, and remarkable hydrothermal stability.[3] However, the materials consisting of pure-silica frameworks are of limited use for various catalytic applications because of the lack of acid sites and ion exchange capacity.

Recently, many efforts have been made to incorporate Al, Ti, and V into the framework of SBA-15, by postsynthesis grafting procedures[4−6] and direct synthesis.[7,8] The postsynthesis method always form the metal oxides in the channels or external surface of the catalysts, which would block the channels and not allow the reactant molecules to access all the reaction sites in the porous matrix.[9] Recently, Vinu et al. have reported the direct synthesis of mesoporous aluminosilicates, AlSBA-15 with variable pore diameters prepared by changing the synthesis temperature.[10−13] These materials possess well-ordered pore structure, high specific pore volume, specific surface area, and large pore diameter. However, the incorporation of Ti into the framework of siliceous mesoporous materials exhibits a range of interesting and useful catalytic properties. The incorporation of Ti onto MCM-41, HMS, MCM-48, and MSU materials has been extensively studied.[14−17] Several researchers also tried to incorporate Ti onto SBA-15 through fluoride-mediated reaction,[18] in microwave hydrothermal conditions,[19] in nonaqueous media,[20] and with other methods,.[21] However, in most of the cases, the efficiency of Ti loading is not always high, especially in direct synthesis, which is expected to provide uniform distribution of heteroatoms in silica structures. In addition, titanium-substituted mesoporous materials with uniform and tunable pore sizes are expected to play an important role in a number of applications, especially the oxidation of small reactant molecules to very bulky molecules. Unfortunately, tuning the pore size of titanium-substituted mesoporous materials has not been studied until now.

Epoxidation is one of the most important industrial reactions for converting hydrocarbons into useful organic intermediates.[22] However, the reaction sometimes requires hazardous chemicals which leave acid waste. Therefore, use of active catalysts with moderate oxidants is enviable to make reaction more eco-friendly. To achieve this, a synthetic zeolite, TS-1 in which a small number of Ti atoms substitute tetrahedral Si atoms in a purely siliceous framework with the MFI structure, has been used.[23] Other Ti-containing crystalline silicates with 12-ring channels, such as Ti-Beta,[24] TAPOS-5,[25] Ti-MOR,[26] and ITQ-

* To whom correspondence should be addressed. Phone: +81-29-851-3354 (Ext. 8679). Fax: +81-29-860-4706. E-mail: vinu.ajayan@nims.go.jp.
† ICYS.
‡ Yokohoma National University.
§ NIMS.

10.1021/jp055851d CCC: $33.50
Published on Web 12/16/2005

7,[27] have been prepared by either direct or postsynthesis method. Among the microporous titanium-substituted materials, Ti-Beta has shown remarkable activity even using the bulky organic oxidant *tert*-butylhydroperoxide (TBHP), which would contribute to the recycling of the *tert*-butyl alcohol. However, these materials still do not satisfy the demands from the fine chemical and pharmaceutical industry, because greater accessibility for reaction space is requested.

In this paper, we report on the direct syntheses and characterization of TiSBA-15 mesoporous molecular sieves with high Ti content (up to Si/Ti = 1.9) under various acid concentrations and synthetic temperatures and their oxidative performance in the styrene epoxidation. It has been found that the amount of Ti content in TiSBA-15 can easily be controlled by the simple adjustment of the molar ratio of water to hydrochloric acid. The pore size of the TiSBA-15 materials can easily be tuned from 8.8 to 12.6 nm by increasing the crystallization temperature without addition of any organic swelling agents. In addition, the environment of Ti atoms doped in SBA-15 materials has been investigated using UV−vis diffuse reflection spectroscopy.

Experimental Section

Materials. Titanium isopropoxide and tetraethyl orthosilicate (TEOS) (Merck) were used as the source for titanium and silicon, respectively. Triblock copolymer poly(ethylene glycol)-*block*-poly(propylene glycol)-*block*-poly(ethylene glycol) (Pluronic P123, molecular weight = 5800, $EO_{20}PO_{70}EO_{20}$; Aldrich) was used as the structure-directing template. Styrene, hydrogen peroxide, and TBHP were purchased from Merck and used without further purification.

Syntheses of TiSBA-15. TiSBA-15 samples with different n_{Si}/n_{Ti} ratios were synthesized using poly(ethylene glycol)-*block*-poly(propylene glycol)-*block*-poly(ethylene glycol) as a structure-directing agent with the following molar gel composition: TEOS/0.14−0.35 Ti(-O^{i}Pr)$_4$/0.016 P123/0.46−5.54 HCl/127−190 H_2O. In a typical synthesis, 4 g of pluronic P123 was added to 30 mL of water. After stirring for a few hours, a clear solution was obtained. Thereafter, the required amount of HCl was added and the solution was stirred for another 2 h. Then, 9 g of tetraethyl orthosilicate and the required amount of the desired Ti source were added, and the resulting mixture was stirred for 24 h at 40 °C. A first set of samples was prepared by changing the molar ratio of water to hydrochloric acid and denoted as TiSBA-15(*x*H), where *x* denotes the molar water to hydrochloric acid ratio (n_{H_2O}/n_{HCl}). For this set of samples, the n_{Si}/n_{Ti} ratio in the gel was fixed to 7. A second set of samples was prepared by using a fixed molar water to hydrochloric acid ratio of 276 (70 mL of 0.29 M HCl) and a n_{Si}/n_{Ti} ratio of 7 while varying the synthesis temperature from 100 to 130 °C. The samples were labeled TiSBA-15-*y*T, where *y* denotes the synthesis temperature. The solid products were recovered by filtration, washed several times with water, and dried overnight at 100 °C. The resulting gel was transferred to the polypropylene bottle and kept in an air oven at 100 °C for 48 h. The solid product was recovered by filtration, washed with water several times, and dried overnight at 100 °C. Finally, the product was calcined at 540 °C to remove the template.

Characterization. The powder X-ray diffraction patterns of TiSBA-15materials were collected on a Siemens D5005 diffractometer using Cu Kα (k = 0.154 nm) radiation. The diffractograms were recorded in the 2θ range of 0.7−10° with a 2θ step size of 0.01° and a step time of 10 s. Nitrogen adsorption and desorption isotherms were measured at 196 °C on a Quantachrome Autosorb 1 sorption analyzer. The samples were outgassed for 3 h at 250 °C under vacuum in the degas port of the adsorption analyzer. The specific surface area was calculated with use of the Brunauer−Emmett−Teller (BET) method. The pore size distributions were obtained from the adsorption and desorption branch of the nitrogen isotherms by the Barrett−Joyner−Halenda method. UV−vis diffuse reflectance spectra were measured with a Perkin-Elmer Lambda 18 spectrometer equipped with a Praying-Mantis diffuse reflectance attachment. $BaSO_4$ was used as reference. Elementary analysis was done using an Analyst AA 300 spectrometer.

TABLE 1: Synthesis Condition and Ti Content of Calcined TiSBA-15 Samples

				n_{Si}/n_{Ti} ratio	
catalyst	n_{H_2O}/n_{HCl}	synth temp/°C	a_0/(nm)	gel	product
TiSBA-15(33H)	33	100	10.61	7	155.6
TiSBA-15(68H)	68	100	10.73	7	76.8
TiSBA-15(137H)	137	100	10.94	7	28.3
TiSBA-15(276H)	276	100	11.54	7	6.1
TiSBA-15-110T	276	110	12.52	7	6.0
TiSBA-15-120T	276	120	12.16	7	6.8
TiSBA-15-130T	276	130	12.74	7	7.6

Catalytic Studies. Anhydrous analytical grade chemicals were used without further purification. The liquid-phase epoxidation of styrene with hydrogen peroxide or TBHP was carried out in a 50 mL two-necked flask attached to a condenser and a septum. The temperature of the reaction vessel was maintained using an oil bath. The reaction condition for the styrene epoxidation by hydrogen peroxide can be described as follows: 7.5 mmol; 31 wt % H_2O_2, 7.5 mmol; catalyst, 50 mg; MeCN, 10 mL; reaction time, 4 h; reaction temperature, 60 °C. Similarly, the styrene epoxidation was carried out under the following condition: styrene, 7.5 mmol; 70 wt % TBHP, 7.5 mmol; catalyst, 50 mg; MeCN, 10 mL; reaction time, 4 h; reaction temperature, 60 °C.

Results and Discussion

The n_{Si}/n_{Ti} atomic ratios of the TiSBA-15 materials prepared at different molarn_{H_2O}/n_{HCl} are given in Table 1. The initial n_{Si}/n_{Ti} ratio was fixed to 7 in the synthesis gel. It can be seen from the Table 1 that the n_{Si}/n_{Ti} of the product decreases from 155.6 to 6.1 with increasing n_{H_2O}/n_{HCl} ratio. At high n_{H_2O}/n_{HCl} ratio, the n_{Si}/n_{Ti} atomic ratios in the products are close to the ratios in the corresponding gel. This characteristic of the materials prepared here is apparently different from metal-substituted SBA-15, especially, TiSBA-15 materials in the other literatures[28] and SBA-15 materials with Al[10−13] and Fe[29] prepared in our laboratory. SBA-15 materials can generally be synthesized under strongly acidic hydrothermal conditions that easily induce the dissociation of the Ti−O−Si bonds. The hydrolysis of titanium alkoxides is virtually instantaneous, whereas the hydrolysis of silicon precursors is much slower. Lowering the acidity of the solution may decrease the hydrolysis rate of the titanium precursors to match that of the silicon precursors. This might enhance the interaction between the Ti−OH and Si−OH species in the synthesis gel resulting in a higher amount of Ti incorporation at high n_{H_2O}/n_{HCl} ratio. The results listed in Table 1 apparently show that a decrease of acid concentration induced a high loading of Ti in the SBA-15 structure, which was probably caused by suppressed Ti−O−Si cleavage and moderated hydrolysis of titanium alkoxide.

The powder XRD patterns of TiSBA-15 samples prepared using different molar ratios of water to hydrochloric acid (n_{H_2O}/n_{HCl}) are shown in Figure 1. The well-defined XRD patterns are similar to those recorded for all-silica SBA-15 materials as

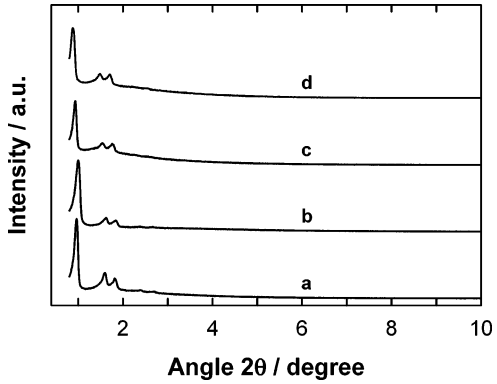

Figure 1. XRD powder patterns of TiSBA-15 materials prepared at different n_{H_2O}/n_{HCl} ratios: (a) TiSBA-15(276H), (b) TiSBA-15(137H), (c) TiSBA-15(68H), and (d) TiSBA-15(33H).

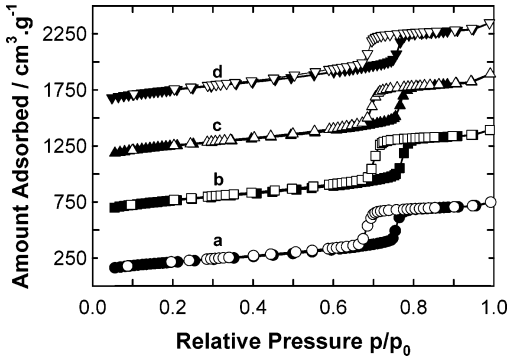

Figure 2. Nitrogen adsorption isotherms of TiSBA-15 materials prepared at different n_{H_2O}/n_{HCl} ratios: (closed symbols, adsorption; open symbols, desorption): (●) TiSBA-15(276H), (■) TiSBA-15(137H), (▲) TiSBA-15(68H), and (◆) TiSBA-15(33H).

described by Zhao et al.[3] The XRD patterns of all TiSBA-15 materials exhibit five well-resolved peaks which are indexed to the (100), (110), (200), (210), and (300) reflections of the hexagonal space group *P*6*mm*. The length of the hexagonal unit cell a_0 is calculated using the formula $a_0 = 2d_{100}/\sqrt{3}$. The observed *d* spacings are compatible with the hexagonal *P*6*mm* space group. It is interesting to note that the length of the unit cell a_0 increases from 10.61 to 11.54 nm with increasing n_{H_2O}/n_{HCl} molar ratio from 33 to 276. Moreover, the amount of Ti incorporation in the materials also increases with increasing n_{H_2O}/n_{HCl} molar ratio. The increase of the unit cell parameter and the amount of Ti incorporation with increasing n_{H_2O}/n_{HCl} ratio indicates the presence of Ti atoms in the framework. All the above results suggest that the amount of Ti incorporation can easily be controlled by the simple adjustment of the molar n_{H_2O}/n_{HCl} ratio without affecting the structural order of the parent SBA-15 materials.

The nitrogen adsorption−desorption isotherms of the corresponding samples are shown in Figure 2. They exhibit isotherms of type IV of the IUPAC classification featuring a narrow step due to capillary condensation of N_2 in the primary mesopores. A steep increase and a H1-type hysteresis loop occur in the isotherms due to the capillary condensation and desorption of nitrogen, which strongly suggest the presence of large mesopores in these TiSBA-15 materials. Pore size distribution profiles shown in Figure 1S (see Supporting Information) reveal that a change in acid concentration does not virtually affect the pore size distribution though the n_{Si}/n_{Ti} ratio varies between 6 and 155. Analyzed pore geometries are summarized in Table 2, where high BET surface area (ca. 900 $m^2\ g^{-1}$) and large specific pore volume (1.1−1.3 $cm^3\ g^{-1}$) can be seen together with a large pore diameter of ca. 9 nm for all the corresponding samples. These results indicate that the Ti loading can be controlled in SBA-15 materials while maintaining even the textural parameters and pore structure through control of the acid concentration of the synthetic gels.

TABLE 2: Texture Parameters of Calcined TiSBA-15 Samples

catalyst	$A_{BET}/(m^2\ g^{-1})$	dp, BJH/(nm)	$V_p/(cm^3\ g^{-1})$
TiSBA-15(33H)	773	8.8	1.1
TiSBA-15(68H)	957	9.3	1.3
TiSBA-15(137H)	914	9.3	1.3
TiSBA-15(276H)	916	9.0	1.2
TiSBA-15(4)	802	7.4	1.0
TiSBA-15(2)	757	8.6	1.0
TiSBA-15-110T	809	10.7	1.3
TiSBA-15-120T	584	11.9	1.3
TiSBA-15-130T	555	12.6	1.3

For more specific information about the surrounding environment of Ti atoms in the SBA-15 framework, UV−vis diffuse reflectance spectroscopy (UV−vis DRS) was performed.[30,31] A band with a maximum at about 200−240 nm is attributed to a ligand-to-metal charge-transfer transition in isolated TiO_4 or $HOTiO_3$ units, which is the direct evidence for titanium atoms incorporated into the framework of the mesoporous silica. Another band centered at about 330 nm is typical of ligand-to-metal charge transfer, which is a sign of the presence of bulk titania.[32] A band between these absorptions, such as a band centered at ca. 270 or 280 nm, can be assigned to penta or hexacoordinated Ti species, which are most likely generated through hydration of the tetrahedrally coordinated sites.[33−35]

Figure 3A displays the UV−vis DR spectra of as-synthesized TiSBA-15 samples prepared at different n_{H_2O}/n_{HCl} ratios. All the samples except TiSBA-15(33H) show a broad band between 240 and 340 nm, centered at 280 nm. This band can be attributed to solvent or water molecules coordinated to the isolated Ti species which are originated from either the incomplete condensation or partial polymerization.[33−35] It should be noted that the intensity of the peak is rising with increasing the n_{H_2O}/n_{HCl}, confirming the increase of Ti loading at high n_{H_2O}/n_{HCl} ratio. For the sample prepared at $n_{H_2O}/n_{HCl} = 33$, TiSBA-15-(33H) gives a broad band between 260 and 400 nm, centered around 330 nm, which may be attributed to the anatase-like TiO_2 particles which are formed through partial condensation.[32] Figure 3B shows the UV−vis DR spectra of calcined TiSBA-15 samples prepared at n_{H_2O}/n_{HCl} ratios. It is interesting to note that the intensity of all peaks is significantly increased upon calcination. The TiSBA-15(276H) shows a shift in the peak position from 280 to 245 nm upon calcinations, whereas no change in the peak position is observed for other samples. The peak around 245 nm is generally assigned to a low-energy charge-transfer transition of tetrahedral oxygen ligands and central Ti^{4+} ions.[36] The absence of the peak around 330 nm for TiSBA-15(276H) suggests that no bulk titania is found in the TiSBA-15(276H) sample. The above results reveal that the framework incorporation of Ti in SBA-15 is possible in acidic medium synthesis and can be controlled by simple adjustment of the n_{H_2O}/n_{HCl} ratio.

Further increase of the Ti content was carried out by changing the n_{Si}/n_{Ti} ratio in the gel at a fixed n_{H_2O}/n_{HCl} ratio of 276. The elemental compositions of TiSBA-15 materials synthesized with different n_{Si}/n_{Ti} ratios are listed in Table 3. In all cases, the n_{Si}/n_{Ti} ratio of the calcined materials is lower as compared to the input n_{Si}/n_{Ti} ratio in the synthesis gel, suggesting a preferential incorporation of Ti atoms as compared to silicon. As seen in Table 3 (see TiSBA-15(*X*), $X = 6$, 4, and 2), an

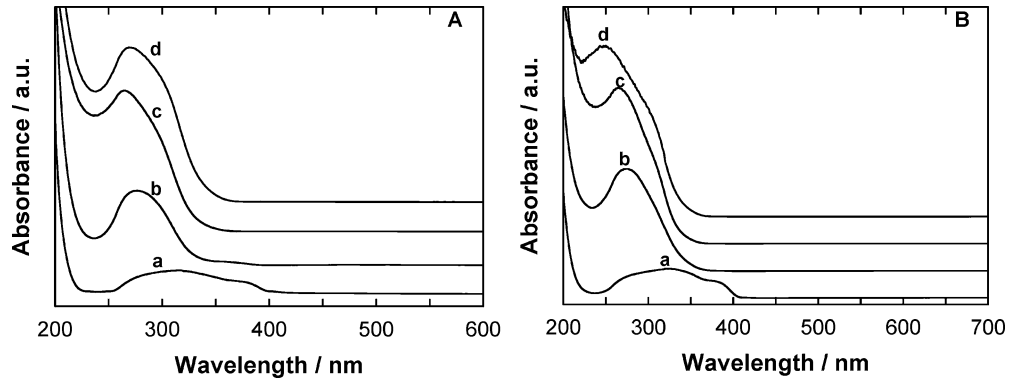

Figure 3. UV−vis DR spectra of (A) as-synthesized and (B) calcined TiSBA-15 materials synthesized at different n_{H_2O}/n_{HCl} ratios: (a) TiSBA-15(276H), (b) TiSBA-15(137H), (c) TiSBA-15(68H), and (d) TiSBA-15(33H).

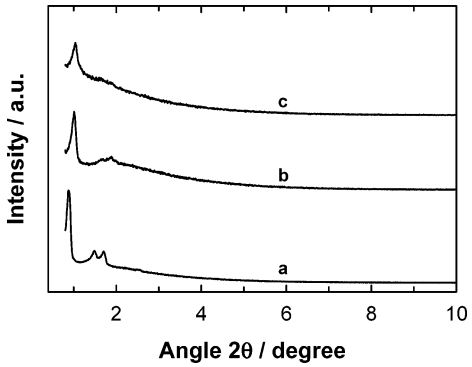

Figure 4. XRD powder patterns of TiSBA-15 materials prepared at different n_{Si}/n_{Ti} ratios: (a) TiSBA-15(6), (b) TiSBA-15(4), and (c) TiSBA-15(2).

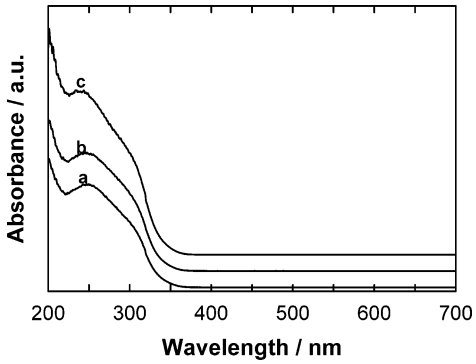

Figure 5. UV−Vis DR spectra of calcined TiSBA-15 materials prepared at different n_{Si}/n_{Ti} ratios: (a) TiSBA-15(6), (b) TiSBA-15-(4), and (c) TiSBA-15(2).

TABLE 3: Structural Parameters of TiSBA-15 Samples with Different n_{Si}/n_{Ti} Ratios

				n_{Si}/n_{Ti} ratio	
catalyst	n_{H_2O}/n_{HCl}	synth temp/°C	a_0/nm	gel	product
TiSBA-15(6)	276	100	11.54	7	6.1
TiSBA-15(4)	276	100	10.08	5	3.6
TiSBA-15(2)	276	100	9.81	3	1.9

increase of Ti content in the synthetic gel efficiently enhanced the Ti content in the product and $n_{Si}/n_{Ti} = 1.9$ was achieved as the highest Ti content. Although (110) and (200) peaks are broadened in the XRD profiles of the high-Ti-content sample (Figure 4), a clear (100) peak still remains. Less sharp profiles in N_2 adsorption−desorption isotherms and broadened pore size distribution profiles for TiSBA-15(4) and TiSBA-15(2) samples (Figures 2S and 3S, see Supporting Information) indicate the pore structures of the high-Ti-content materials are somehow degraded. However, pore geometries of these samples confirm that these materials still keep a high surface area (>750 m^2 g^{-1}) and pore volume (>1.0 cm^3 g^{-1}) with large pore diameters (7.4 and 8.6 nm for TiSBA-15(4) and TiSBA-15(2), respectively). Therefore, the SBA-15 mesoporous materials with very high Ti content can be obtained by adjusting the n_{Si}/n_{Ti} in the synthetic gel under appropriate acidic conditions, although certain degradation of the structural regularity accompanies increasing Ti content in the product.

Figure 5 shows the UV−vis DR spectra of calcined TiSBA-15 samples with different n_{Si}/n_{Ti} ratios. All the samples including TiSBA-15(2), which has a high Ti content among the samples studied, show a broad band between 230 and 340 nm, centered around 245 nm, and the intensity of the band increases with increasing Ti loading. This band is attributed to the charge-transfer transition associated with an isolated Ti^{4+} in tetrahedral

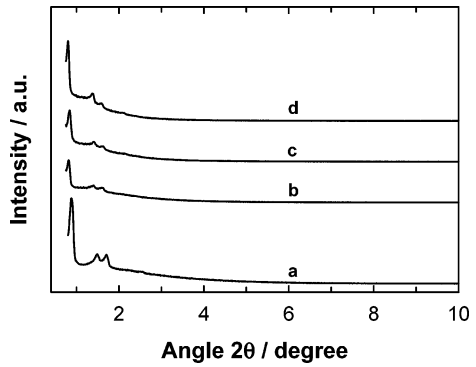

Figure 6. XRD powder patterns of TiSBA-15 materials prepared at different synthesis temperatures: (a) TiSBA-15-100T, (b) TiSBA-15-110T, (c) TiSBA-15-120T, and (d) TiSBA-15-130T.

coordination. These results indicate that most of the Ti atoms occupy a tetrahedral coordination position irrespective of the Ti content in the silica framework of SBA-15 mesoporous molecular sieves synthesized under acidic conditions.

As the independent physical parameter for the TiSBA-15 preparation, the synthetic temperature was modified. The n_{Si}/n_{Ti} ratios in the products are not significantly affected upon changing temperature (Table 1; see TiSBA-15(276H) and TiSBA-15-*y*T (y = 100, 120, and 130)), and the structural regularity as seen in XRD patterns (Figure 6) is kept high for all the samples synthesized at different temperatures. With increasing synthesis temperature, the XRD reflections are shifted to lower 2θ values, reflecting an expansion of the unit cell size (Table 1). The observed d spacings are compatible with the hexagonal *P*6*mm* space group. It can be also seen that the relative intensity of the (110) and (200) refection shifts considerably; the intensity of the (110) reflection increases,

TABLE 4: Epoxidation of Styrene with H_2O_2 over TiSBA-15 Catalysts[a]

		product selectivity		H_2O_2/mol %	
catalyst	conversion/(mol %)	benzaldehyde	styrene oxide	conversion	efficiency
TiSBA-15(6)	16.7	70.4	29.6	23.1	72.3
TiSBA-15(4)	18.1	69.2	30.8	25.7	70.4
TiSBA-15(2)	16.4	68.9	31.1	22.8	71.9

[a] Conditions: styrene, 7.5 mmol; 31 wt % H_2O_2, 7.5 mmol; catalyst, 50 mg; MeCN, 10 mL; reaction time, 4 h; reaction temperature, 60 ° C.

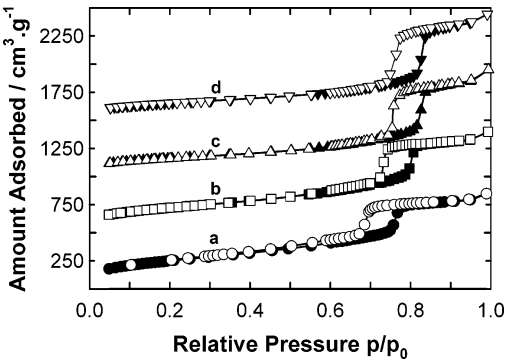

Figure 7. Nitrogen adsorption isotherms of TiSBA-15 materials prepared at different synthesis temperatures: (closed symbols, adsorption; open symbols, desorption): (●) TiSBA-15-100T, (■) TiSBA-15-110T, (▲) TiSBA-15-120T, and (◆) TiSBA-15-130T.

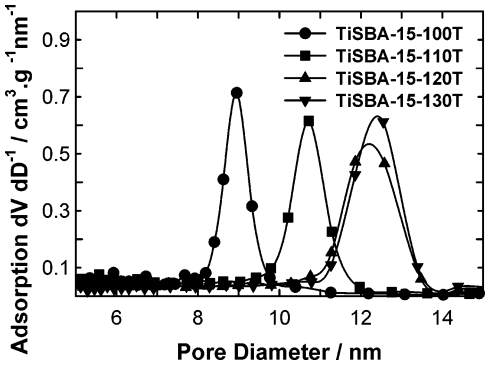

Figure 8. BJH adsorption pore size distributions for the TiSBA-15 materials prepared at different synthesis temperatures: (●) TiSBA-15-100T, (■) TiSBA-15-110T, (▲) TiSBA-15-120T, and (◆) TiSBA-15-130T.

where as the intensity of the (200) reflection decreases. The more intense (110) peak in the TiSBA-15-130T indicates that the material possesses thinner walls, as suggested by Feuston and Higgins[37] for the analogous hexagonal structure of MCM-41. Moreover, the structural order of the material is maintained up to the synthesis temperature of 130 °C.

The N_2 adsorption−desorption isotherms (Figure 7) also show sharp profiles featuring a narrow step due to capillary condensation of N_2 in the primary mesopores. The position of the capillary condensation step shifts to higher relative pressure with increasing synthesis temperature. The most interesting characteristics of the temperature effects were observed for pore size distributions (Figure 8). An increase of the synthetic temperature apparently shifts the pore diameter to a larger region. Pore geometries are also summarized in Table 2. Upon increasing the synthetic temperature from 100 to 130 °C, the pore diameter increased to 12.6 nm at the expense of the pore surface area, while the specific pore volume remained unchanged. These features suggest that the temperature increase would cause a decrease of the micropore population accompanying the pore size increment. The plausible mechanism of this observation can be drawn as follows.[38] The formation of micropores in the SBA-15 synthesis might be explained by sharing their hydration sphere at ethylene oxide headgroups of the template micelles. An increase of synthesis temperature induces partial dehydration of the poly(ethylene oxide) cores. The interactions between the micelles through their poly(ethylene oxide) groups decrease, resulting in the decrease of the microporosity. Dehydration of the micelle increases the portion of hydrophobic core into which the silica precursor does not preferably penetrate. Consequently, pore size increases at higher synthesis temperature.

TABLE 5: Epoxidation of Styrene with TBHP over TiSBA-15 Catalysts[a]

		product selectivity	
catalyst	conversion/(mol %)	benzaldehyde	styrene oxide
TiSBA-15(6)	10.1	52.7	47.3
TiSBA-15(4)	12.7	51.1	48.9
TiSBA-15(2)	10.3	53.3	46.7

[a] Conditions: styrene, 7.5 mmol; 70 wt % TBHP, 7.5 mmol; catalyst, 50 mg; MeCN, 10 mL; reaction time, 4 h; reaction temperature, 60 ° C.

Mesoporous silica materials with doping with heteroatoms such as Ti, Fe, and Al are known as effective catalysts of oxidation of alkenes.[39] For demonstration of catalytic ability of the TiSBA-15 materials prepared in this research, styrene oxidation by hydrogen peroxide (H_2O_2) and TBHP as oxidants was demonstrated. In this reaction, benzaldehyde and styrene oxide are obtained as major products. The results of the styrene oxidation by H_2O_2 are summarized in Table 4. Conversion, product selectivity, and H_2O_2 efficiency were not significantly influenced by Ti content in the catalysts. It was reported that an increase of the Ti content in the mesoporous catalysts decreases epoxide selectivity and H_2O_2 efficiency due to a decrease of isolated Ti atoms in the framework.[40] The absence of such deterioration tendency in our results in Table 4 confirm that a certain amount of isolated Ti atoms is present even at very high Ti content in the SBA-15 framework. It is also suggested by unaltered UV−vis spectra upon Ti content increase, as seen in Figure 5. When TBHP was used as an oxidant (Table 5), the selectivity of styrene oxides (47−49%) was apparently increased compared with those observed in the reaction with H_2O_2 (ca. 30%). It may be caused by disturbance of epoxidation by water in reaction with aqueous H_2O_2.[41] The results obtained here suggest the importance of the selection of the oxidants to achieve desirable product selectivity.

Conclusions

Syntheses of TiSBA-15 mesoporous molecular sieves under various conditions have been investigated. The obtained results clearly show that the Ti content and pore geometries of TiSBA-15 materials are well-controllable by synthetic conditions of acid concentration, gel composition, and temperature. Optimization of acid concentration and Ti content in synthetic gels provide mesoporous TiSBA-15 with very high Ti content up to $n_{Si}/n_{Ti} = 1.9$. Control of the synthetic temperature resulted in tuning of pore geometries while maintaining high structural regularity and high Ti content, and pore size enlargement up to 12.6 nm with a pore volume of 1.3 $cm^3\ g^{-1}$ has been achieved. The nature

and the coordination of Ti atoms in silica frameworks appropriate for catalysis were proved by UV−vis spectroscopy and catalytic reaction and by oxidation of styrene by H_2O_2 and TBHP. The obtained knowledge in this research would be useful in preparing tailored catalysts.

Acknowledgment. A. V. is grateful to the Special Coordination Funds for Promoting Science and Technology from the Ministry of Education, Culture, Sports, Science and Technology of the Japanese Government for the award of an ICYS Research Fellowship. A. V. is also thankful to Mr. T. Sasaki for technical assistance.

Supporting Information Available: Figures showing pore size distributions and nitrogen adsorption−desorption isotherms. This material is available free of charge via the Internet at http://pubs.acs.org.

References and Notes

(1) Beck, J. S.; Vartuli, J. C.; Roth, W. J.; Leonowicz, M. E.; Kresge, C. T.; Schmitt, K. D.; Chu, C. T. W.; Olson, D. H.; Sheppard, E. W.; McCullen, S. B.; Higgins, J. B.; Schlenker, J. L. *J. Am. Chem. Soc.* **1992**, *114*, 10834.

(2) Kresge, C. T.; Leonowicz, M. E.; Roth, W. J.; Vartuli, J. C.; Beck, J. S. *Nature* **1992**, *359*, 710.

(3) Zhao, D. Y.; Huo, Q. S.; Feng, J. L.; Chmelka, B. F.; Stucky, G. D. *J. Am. Chem. Soc.* **1998,** *120*, 6024.

(4) Luan, Z. H.; Hartmann, M.; Zhao, D. Y.; Zhou, W. Z.; Kevan, L. *Chem. Mater.* **1999**, *11*, 1621.

(5) Luan, Z. H.; Bae, J. Y.; Kevan, L. *Chem. Mater.* **2000**, *12*, 3202.

(6) Morey, M. S.; O'Brien, S.; Schwarz, S.; Stucky, G. D. *Chem. Mater.* **2000**, *12*, 898.

(7) Yue, Y. H.; Gedeon, A.; Bonardet, J. L.; Melosh, N.; D'Espinose, J. B.; Fraissard, J. *Chem. Commun.* **1999**, 1967.

(8) Bharat, L. N.; Johnson, O., Sridhar, K. *Chem. Mater.* **2001**, *13*, 552.

(9) Murugavel, R.; Roesky, H. W. *Angew. Chem., Int. Ed. Engl.* **1997**, *36*, 477.

(10) Vinu, A.; Murugesan, V.; Bohlmann, W.; Hartmann, M. *J. Phys. Chem. B* **2004**, *108*, 11496.

(11) Vinu, A.; Kumar, G. S.; Ariga, K.; Murugesan, V. *J. Mol. Catal. A −Chemical* **2005**, *235*, 57.

(12) Vinu, A.; Sawant, D. P.; Ariga, K.; Hartmann, M.; Halligudi, S. B. *Microporous Mesoporous Mater.* **2005**, *80*, 195.

(13) Vinu, A.; Devassy, B. M.; Halligudi, S. B.; Bohlmann, W.; Hartmann, M. *Appl. Catal. A-General* **2005**, *281*, 207.

(14) (a) Kresge, C. T.; Lenowicz, M. E.; Roth, W. J.; Vartuli, J. C. U.S. Patent 5,250,282, 1993. (b) Blasco, T.; Corma, A.; Navarro, M. T.; Pariente, J. P. *J. Catal.* **1995**, *156*, 65. (c) Schuchardt, U.; Cardoso, D.; Sercheli, R.; Pereira, R.; da Cruz, R. S.; Guerreiro, M. C.; Mandelli, D.; Spinacá, E. V.; Pires, E. L. *Appl. Catal. A-Gen.* **2001**, *211*, 1.

(15) (a) Gontier, S.; Tuel, A. *Zeolites* **1995**, *15*, 601. (b) Zhang, W.; Froba, M.; Wang, J.; Tanev, P. T.; Wong, J.; Pinnavaia, T. J. *J. Am. Chem. Soc.* **1996**, *118*, 9164.

(16) (a) Morey, M. S.; O'Brien, S.; Schwarz, S.; Stucky, G. D. *Chem. Mater.* **2000**, *12*, 898. (b) Morey, M.; Davidson, A.; Stucky, G. *Microporous Mater.* **1996**, *6*, 99.

(17) (a) Bagshaw, S. A.; DiRenzo, F.; Fajula, F. *Chem. Commun.* **1996**, 2209. (b) Kim, S. S.; Zhang, W.; Pinnavaia, T. J. *Science* **1998**, *282*, 1302.

(18) Zhang, W.-H..; Lu, J.; Han, B.; Li, M.; Xiu, J.; Ying, P.; Li, C. *Chem. Mater.* **2002**, *14*, 3413.

(19) Newalkar, B. L.; Olanrewaju, J.; Komarneni, S. *Chem. Mater.* **2001**, *13*, 552.

(20) (a) Yang, P.; Zhao, D.; Margolese, D. I.; Chmelka, B. F.; Stucky, S. D. *Nature* **1998**, *396*, 152. (b) Yang, P.; Zhao, D.; Margolese, D. I.; Chmelka, B. F.; Stucky, S. D. *Chem. Mater.* **1999**, *11*, 2813.

(21) Luan, Z.; Maes, E. M.; van der Heide, P. A. W.; Zhao, D.; Czernuszewicz, R. S.; Kevan, L. *Chem. Mater.* **1999**, *11*, 3680. (b) Markowitz, M. A.; Jayasundera, S.; Miller, J. B.; Klaehn, J.; Burleigh, M. C.; Spector, M. S.; Golledge, S. L.; Castner, D. G.; Gaber, B. P. *Dalton* **2003**, 3398. (c) Wu, S.; Han, Y.; Zou, Y.-C.; Song, J.-W.; Zhao, L.; Di, Y.; Liu, S.-Z.; Xiao, F.-Z. *Chem. Mater.* **2004**, *16*, 486. (d) Hua, Z.; Bu, W.; Lian, Y..; Chen, H.; Li, L.; Zhang, L.; Li, C.; Shi, J. *J. Mater. Chem.* **2005**, *15*, 661.

(22) (a) Deubel, D. V.; Frenking, G.; Gisdaki, P S..; Herrmann, W. A.; Rosch, N.; Sundermeyer, J. *Acc. Chem. Res.* **2004**, *37*, 645. (b) Tse, M. K.; Döbler, C.; Bhor, S.; Klawonn, M.; Mägerlein, W.; Hugl, H.; Beller, M. *Angew. Chem., Int. Ed.* **2004**, *43*, 5255. (c) Shi, Y. *Acc. Chem. Res.* **2004**, *37*, 488. (d) Yang, D. *Acc. Chem. Res.* **2004**, *37*, 497. (e) Aggarwal, V. K.; Winn, C. L. *Acc. Chem. Res.* **2004**, *37*, 611. (f) Hickey, M.; Goeddel, D.; Crane, Z.; Shi, Y. *Proc. Natl. Acad. Sci. U.S.A.* **2004**, *101*, 5794. (g) McGiarrigle E. M.; Gilheany D. G. *Chem. Rev.* **2005**, *105*, 1563.

(23) (a) Hutter, R.; Mallat, T.; Baiker, A. *J. Catal.* **1995**, *157*, 665. (b) Notari, B. *Adv. Catal.* **1996**, *41*, 253. (c) Vayssilov, G. N. *Catal. Rev. Sci. Eng.* **1997**, *39*, 209. (d) Corma, A.; Garcia, H. *Chem. Rev.* **2002**, *102*, 3837.

(24) (a) Camblor, M. A.; Constantini, M.; Corma, A.; Esteve, P.; Gilbert, L.; Martinez, A.; Valencia, S. *Appl. Catal. A-Gen.* **1995**, *133*, L185. (b) Jappar, N.; Xia, Q.; Tatsumi, T. *J. Catal.* **1998**, *180*, 132. (c) Coles, M. P.; Lugmair, C. G.; Terry, K. W.; Tilley, T. D. *Chem. Mater.* **2000**, *12*, 122.

(25) Tuel, A. *Zeolites* **1995**, *15*, 228.

(26) (a) Wu, P.; Tatsumi, T.; Komatsu, T.; Yashima, T. *J. Catal.* **2001**, *202*, 245. (b) Wu, P.; Tatsumi, T. *Catal. Surv. Asia* **2004**, *8*, 137.

(27) (a) Díaz-Cabaña, M. J.; Villaescusa, L. A.; Camblor, M. A. *Chem. Commun.* **2000**, 761. (b) Corma, A, Díaz-Cabaña, M. J.; Domine, M. E.; Rey, F. *Chem. Commun.* **2000**, 1725.

(28) (a) Wu, P.; Tatsumi, T.; Komatsu, T.; Yashima, T. *Chem. Mater.* **2002**, *14*, 1657. (b) Zhang, W.-H.; Lu, J.; Han, B.; Li, M.; Xiu, J.; Ying, P.; Li, C. *Chem. Mater.* **2002**, *14*, 3413. (c) Chen, Y.; Huang, Y.; Xiu, J.; Han, X.; Bao, X. *Appl. Catal. A-Gen.* **2004**, *273*, 185.

(29) Vinu, A.; Sawant, D. P.; Hossain, K. Z.; Ariga, K.; Hartmann, M.; Nomura, M. *Chem. Mater.* **2005**, *17*, 5339.

(30) (a) Thomas, J. M. *Top. Catal.* **2001**, *15*, 85. (b) Volta, J.-C. *Top. Catal.* **2001**, *15*, 121. (c) Yang, Y.; Han, Y.; Lin, K.; Tian, G.; Feng, Y.; Meng, X.; Di, Y.; Du, Y.; Zhang, Y.; Xiao, F.-S. *Chem. Commun.* **2004**, 2612.

(31) (a) Luan, Z.; Kevan, L. *J. Phys. Chem. B* **1997**, *101*, 2020. (b) Wu, P.; Tatsumi, T.; Komatsu, T.; Yashima, T. *J. Phys. Chem. B* **2001**, *105*, 2897. (c) Trukhan, N. N.; Romannikov, V. N.; Shmakov, A. N.; Vanina, M. P.; Paukshtis, E. A.; Bukhtiyarov, V. I.; Kriventsov, V. V.; Danilov, I. Y.; Kholdeeva, O. A. *Microporous Mesoporous Mater.* **2003**, *59*, 73.

(32) Klaas, J.; Schulz-Ekloff, G.; Jaeger, N. I. *J. Phys. Chem. B* **1997,** *101*, 1305.

(33) Tozzola, G.; Mantegazza, M. A.; Ranghino, G.; Petrini, G.; Bordiga, S.; Ricchiardi, G.; Lamberti, C.; Zulian, R.; Zecchina, A. *J. Catal.* **1998,** *179*, 64.

(34) Geobaldo, F.; Bordiga, S.; Zecchina, A.; Giamello, E.; Leofanti, G.; Petrini, G. *Catal. Lett.* **1992,** *16*, 109.

(35) Sinclair, P. E.; Sankar, G.; Richard, C.; Catlow, A.; Thomas, J. M.; Maschmeyer, T. *J. Phys. Chem. B* **1997**, *101*, 4232.

(36) Trukhan, N. N.; Romannikov, V. N.; Paukshtis, E. A.; Shmakov, A. N.; Kholdeeva, O. A. *J. Catal.* **2001**, *202*, 110.

(37) Feuston, B. P.; Higgins, J. B. *J. Phys. Chem.* **1994**, *98*, 4459.

(38) (a) Galarneau, A.; Cambon, H.; Di Renzo, F.; Fajula, F. *Langmuir* **2001**, *17*, 8328. (b) Hartmann, M.; Vinu, A. *Langmuir* **2002,** *18*, 8010.

(39) (a) Corma, A.; Diaz, U.; Domine, M. E.; Fornés, V. *J. Am. Chem. Soc.* **2000**, *122*, 2804. (b) Wang, Y.; Zhang, Q.; Shishido, T.; Takehira, K. *J. Catal.* **2002**, *209*, 186. (c) Calleja, G.; van Grieken, R.; García, R.; Melero, J. A.; Iglesias, J. *J. Mol. Catal. A-Chem.* **2002**, *182*, 215. (d) Tuel, A.; Hubert-Pfalzgraf, L. G. *J. Catal.* **2003**, *217*, 343. (e) Meng, X.; Li, D.; Yang, X.; Yu, Y.; Wu, S.; Han, Y.; Yang, Q.; Jiang, D.; Xiao, F.-S. *J. Phys. Chem. B* **2003**, *107*, 8972. (f) Chiker, F.; Nogier, J. P.; Launay, F.; Bonardet, J. L. *Appl. Catal. A-Gen.* **2003**, *243*, 309. (g) Chiker, F.; Launay, F.; Nogier, J. P.; Bonardet, J. L. *Green Chem.* **2003**, *5*, 318. (h) Chen, Y.; Huang, Y.; Xiu, J.; Han, X.; Bao, X. *Appl. Catal. A-Gen.* **2004**, *273*, 185. (i) Lapisardi, G.; Chiker, F.; Launay, F.; Nogier, J.-P.; Bonardet, J.-L. *Catal. Commun.* **2004**, *5*, 277. (j) Ji, D.; Zhao, R.; Lv, G.; Qian, G.; Yan, L.; Suo *J. Appl. Catal. A-Gen.* **2005**, *281*, 39.

(40) Yu, J.; Feng, Z.; Xu, L.; Li, M.; Xin, Q.; Liu, Z.; Li, C. *Chem. Mater.* **2001**, *13*, 994.

(41) (a) Sheldon, R. A. *J. Mol. Catal.* **1980**, *7*, 107. (b) Jarupatrakorn, J.; Tilley, T. D. *J. Am. Chem. Soc.* **2002**, *124*, 8380.